Volume 12
Number 29
7 August 2024
Pages 17733–18614

Journal of Materials Chemistry A

Materials for energy and sustainability

rsc.li/materials-a

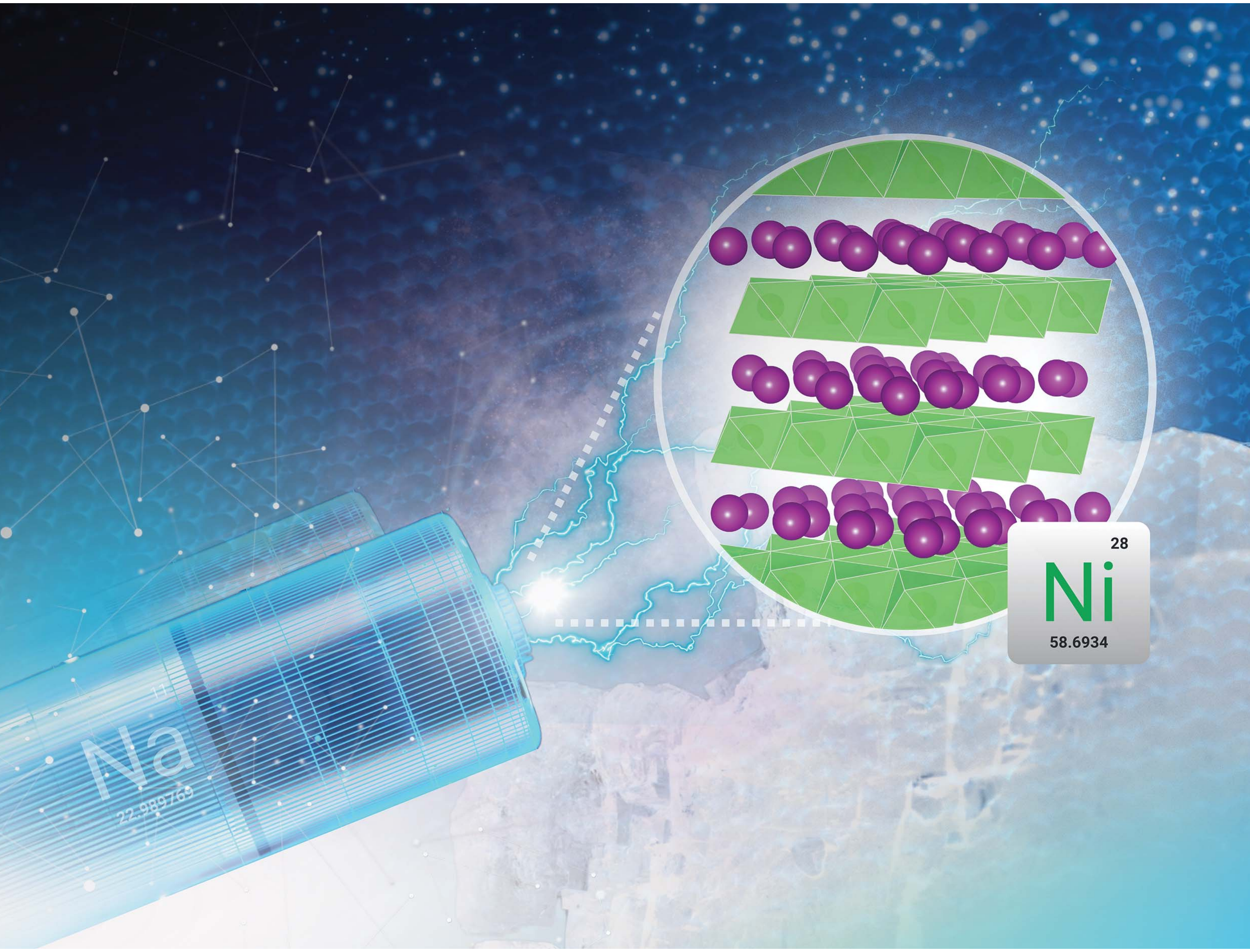

ISSN 2050-7488

ROYAL SOCIETY OF CHEMISTRY

HIGHLIGHT
Josué M. Gonçalves, Hudson Zanin *et al.*
Ni-rich layered cathodes in sodium-ion batteries: perspectives or déjà vu?

Journal of
Materials Chemistry A

HIGHLIGHT

View Article Online
View Journal | View Issue

Cite this: *J. Mater. Chem. A*, 2024, **12**, 17756

Received 25th March 2024
Accepted 28th June 2024

DOI: 10.1039/d4ta01989j

rsc.li/materials-a

Ni-rich layered cathodes in sodium-ion batteries: perspectives or déjà vu?

Josué M. Gonçalves, *[a] Gustavo T. M. Silva [b] and Hudson Zanin *[c]

Sodium-ion batteries (SIBs) are emerging as promising energy storage devices due to the widespread availability of low-cost sodium and their electrochemical mechanism, which bears similarities to lithium-ion batteries (LIBs). The promising potential of Ni-rich layered oxides, coupled with the sense of déjà vu from the advancements seen in LIBs, strongly suggests the practical application of these compounds in SIBs. For the first time, the recent advancements in cathode materials for SIBs are highlighted, focusing on Ni-rich layered transition metal oxides such as $NaNi_xCo_yMn_zO_2$ (Na-NCM), $NaNi_xCo_yAl_zO_2$ (Na-NCA), $Na{-}Ni_xFe_yMn_zO_2$ (Na-NFM) and $NaNi_xCo_yMn_z[TM]_{1-x-y-z}O_2$ (Na-NCM[TM], TM = other transition metal) with $x \geq 0.60$ ($x + y + z = 1$). These materials offer practical synthesis methods, impressive specific capacity, and environmental friendliness. However, challenges remain, including energy density and cycle life. Strategies to engineer high-energy-density SIBs are being pursued, notably developing Ni-rich layered oxide cathode materials. In conclusion, an outlook that assesses the strengths and limitations of this field is pointed out, providing valuable insights to steer future research efforts toward enhancing Ni-rich cathodes, thereby paving the way for further advancements.

1. Introduction

Sodium-ion batteries (SIBs) are emerging as promising candidates as energy storage devices, primarily owing to the widespread availability of low-cost sodium and their electrochemical mechanism, which closely parallels that of commercially prevalent lithium-ion batteries.[1] Furthermore, considering the increasing demand for electromobility, there is a concentrated

Josué M. Gonçalves

Josué Martins Gonçalves is a Researcher at the Mackenzie Institute for Research in Graphene and Nanotechnologies (MackGraphe) within the Mackenzie Presbyterian Institute, Brazil. He graduated in Chemistry at University Vale do Acaraú (UVA) in 2014 and received his PhD from the Institute of Chemistry at the University of Sao Paulo (USP) in 2019. He developed cutting-edge research during his postdoctoral internships at USP (2019–2021), the University of Illinois-Chicago (UIC, 2021–2022), and the University of Campinas (Unicamp, 2023–2024). His current research interests include applications of high-entropy materials for sensors, electrocatalysis, energy conversion, and storage devices.

Gustavo T. M. Silva

Gustavo Thalmer M. Silva obtained his undergraduate degree in Chemistry from the State University of Rio Grande do Norte (2012) and a Master's degree in Chemistry from the Federal University of Rio Grande do Norte (2014). He received his PhD at the Institute of Chemistry of the University of São Paulo (IQ-USP) in 2019 under the supervision of Frank H. Quina and is currently conducting postdoctoral research at the same institution. His research interests include energy sources, colloid and materials chemistry, the chemistry and photochemistry of natural pigments and their synthetic analogues, and quantum chemical methodology for electronically excited states.

---

[a] Mackenzie Institute for Research in Graphene and Nanotechnologies (MackGraphe), Mackenzie Presbyterian Institute, São Paulo, SP, Brazil. E-mail: josue.goncalves@mackenzie.br

[b] Instituto de Química, Universidade de São Paulo, Av. Lineu Prestes 748, Cidade Universitária, São Paulo, SP, Brazil

[c] Advanced Energy Storage Division, Carbon Sci-Tech Labs, Center for Innovation on New Energies, School of Electrical and Computer Engineering, University of Campinas, Av Albert Einstein 400, Campinas, SP 13083-852, Brazil. E-mail: hzanin@unicamp.com.br

effort to expedite the development of new rechargeable batteries or enhance existing materials in current devices. This endeavor is aimed at strengthening electrochemical properties while simultaneously lowering overall costs in accordance with various national policies that have been mandated and implemented. Moreover, the availability of lithium (Li) and cobalt (Co), typically utilized in lithium-ion batteries (LIBs), is severely limited in the Earth's crust.[2] The high cost associated with lithium, coupled with its substantial consumption, presents a significant barrier to the widespread adoption of LIBs in the future.[2] In that regard, SIBs present a notable alternative to LIBs due to the comparable physicochemical properties of sodium to lithium.[3] Additionally, sodium resources are abundantly available on Earth to supplant LIBs for large-scale applications in the near future.[3]

Cathode materials play a crucial role in SIBs, exerting a significant influence on their electrochemical performance, cost, and energy density.[3,4] The primary cathode candidates for SIBs encompass polyanionic compounds, Prussian blue analogues (PBAs), organic materials, and layered transition metal oxides (NaTMOs).[4] Among these, NaTMOs stand out as promising cathode materials for SIBs due to their practical synthesis methods, impressive specific capacity, excellent rate capability, environmentally friendly characteristics, and cost-effectiveness.[3,4] However, the practical implementation of these cathodes faces considerable challenges, particularly concerning energy density and cycle life, especially under extreme temperature conditions.[3]

Fortunately, the scientific community has been diligently crafting strategies to engineer high-energy-density SIBs that can cater to the needs of our energy-hungry society in energy transition. In the realm of designing NaTMOs for SIBs, the landscape appears to evoke a sense of déjà vu reminiscent of advancements seen in well-established LIB technologies. This suggests that the quest for high-performance SIB cathodes based on NaTMOs did not commence from square one; rather, given the striking structural parallels, researchers in the energy storage domain seem to have encountered similar challenges previously. In fact, among recent approaches, the development of nickel-rich (Ni-rich) and cobalt-deficient (Co-free or Co-less) layered materials stands out as a promising trend for fabricating next-generation cathode materials for SIBs. These materials present exceptional energy density, make use of plentiful resources, and exhibit environmental sustainability. Indeed, this approach seeks to mitigate the drawbacks associated with the high cost and supply uncertainty of cobalt, as well as the structural and thermal instability of $NaNiO_2$ in deeply desodiated states and its highly unstable with the electrolyte.[5] Therefore, considering the information provided earlier, there has been a clear upward trajectory in publications on this subject in recent years, indicating that the utilization of Ni-rich-based cathodes in SIBs represents one of the latest perspectives in the realm of cathode materials.

Currently, numerous studies have focused on the fundamental material and chemical challenges associated with layered oxides for SIBs.[3] In fact, several solutions have been proposed to tackle these issues.[3] Besides, many previous reviews extensively discussed the progress and trends on layered oxides for SIBs. For instance, some recent works summarize progress towards specific phases and compositions as cathodes for SIBs such as P2-$Na_{2/3}Ni_{1/3}Mn_{2/3}O_2$,[6] O3-type $Na_xNi_yFe_zMn_{1-y-z}O_2$,[7] $NaNi_xMn_yCo_zO_2$,[8] *etc.* On the other hand, many other comprehensive reviews highlight recent research, development, challenges, and strategies toward the practical application of NaTMO cathodes for SIBs.[3,9] For instance, Li *et al.*[10] reviewed the advancements in NaTMO cathodes for SIBs, primarily encompassing Mn-based layered cathode materials, featuring chemistry ranging from unary to ternary compounds.

To our knowledge, there is currently no comprehensive work detailing the highly promising outcomes of Ni-rich NaTMOs,

Hudson Zanin

Hudson Zanin is a Professor at the School of Electrical and Computer Engineering of the University of Campinas, Brazil, and a Researcher in the Advanced Energy Storage Division of the Center for Innovation on New Energies. His research focuses on developing functional (nano) materials and their application in Energy Storage and Conversion Devices. He has experience in supercapacitors, batteries, and fuel cells' materials and devices. He is the founder of the first South America Lab-scale batteries and supercapacitors manufacturing. Dr Zanin has a PhD degree in Electrical Engineering from the University of Campinas (2012).

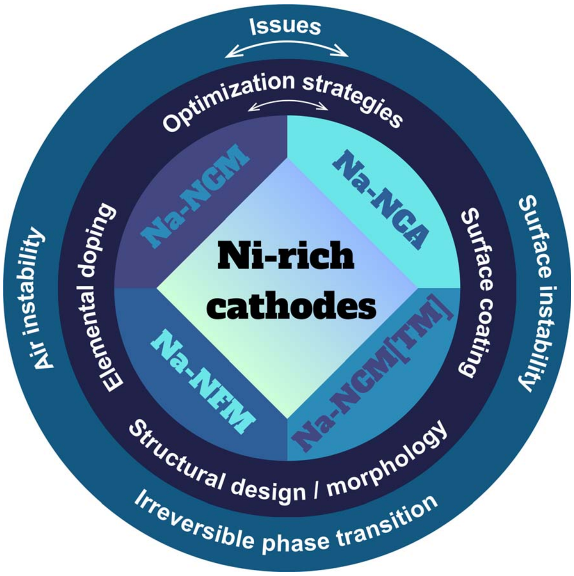

Scheme 1 Main issues and optimization strategies used in the design of Ni-rich $NaNi_xCo_yMn_zO_2$ (Na-NCM), $NaNi_xCo_yAl_zO_2$ (Na-NCA), Na–$Ni_xFe_yMn_zO_2$ (Na-NFM) and $NaNi_xCo_yMn_z[TM]_{1-x-y-z}O_2$ (Na-NCM [TM]) with $x \geq 0.60$ ($x + y + z = 1$).

especially focusing on a complete analysis of the hot topic Ni-rich cathodes based on $NaNi_xCo_yMn_zO_2$ (Na-NCM), $NaNi_xCo_yAl_zO_2$ (Na-NCA), Na–$Ni_xFe_yMn_zO_2$ (Na-NFM) and $NaNi_xCo_yMn_z[TM]_{1-x-y-z}O_2$ (Na-NCM[TM], TM = other transition metal) with $x \geq 0.60$ $(x + y + z = 1)$. Therefore, this Highlight aims to delve into the recent advancements in the design of Ni-rich cathode materials such as Na-NCM, Na-NCA, Na-NFM, and Na-NCM[MT]. It comprehensively summarizes effective strategies employed in the rational design of Ni-rich NaTMO cathodes for SIBs (Scheme 1). This trend seems to evoke a sense of déjà vu, reminiscent of advancements observed in well-established LIB technologies. However, some distinct peculiarities specific to this promising application are highlighted. Additionally, the strengths and weaknesses of this field, offering valuable insights to steer future research efforts toward the development of enhanced Ni-rich NaTMOs, are evaluated.

2. Transition metal layered oxide in SIBs: structure, properties, and challenges

The potential for SIBs as a sustainable alternative to LIBs is indeed strongly promising. However, to enable their applications as high-power energy storage systems, parameters correlated to their electrodes, such as charge and discharge rate (power density), specific capacity (energy density), and cycle life, still need to be improved.[11,12] As well as in LIBs, the cathode material is considered the critical component for determining the electrochemical performance in SIBs, playing a central role in determining the sodium diffusion, energy density, reversibility, and cycle life.[13,14] In addition, the entire cost of SIBs is highly dependent on the cathode material.[11,15] Therefore, it is crucial to develop electrode materials with high capacity that are suitable for practical applications and commercialization.

Although SIBs and LIBs share the same architecture, cell fabrication steps, and working mechanisms and components,[15] directly replicating a cathode material designed for lithium-ion devices for use in SIBs presents challenges, as Na^+ has a larger ionic radius than Li^+, in addition to differences in their chemistry.[11] However, due to the extensive research knowledge in LIBs, a significant amount of mature LIB technology has been adapted for SIBs. As a result, developing sodium analogs of existing LIB electrodes has become a common design approach for SIB electrodes.[15,16] Nonetheless, maintaining a stable structure and enhancing the electrochemical performance of the cathode material to meet the requirements of practical applications remains a challenge.[11] Current SIB cathodes face challenging issues such as undesirable phase changes during cycling, sluggish Na^+ mobility, and unfavorable interface reactions between the electrode and electrolytes.[4,12] These issues are primarily associated with the larger size of Na^+ compared to Li^+, resulting in lower energy density.[12] Therefore, selecting cathode materials that offer good safety, cost-effectiveness, high energy and power densities, and long cycle life and are capable of buffering the repeated (de)insertion of Na^+ is crucial.[12]

Among the most studied cathode materials for SIBs,[12] Na_xTMO_2 ($0 < x \leq 1$, TM represents single or multiple transition-metal elements) has emerged as one of the most important and promising options due to their superior volumetric energy density, high power density, high operating potential, ease of synthesis and non-toxicity.[10,12–14,17] In addition, since lithium layered transition metal oxides (Li_xTMO_2) are the main cathode materials for commercial LIBs, the adoption of Na_xTMO_2 presents higher industrial feasibility, as they can leverage established technologies from mature LIBs, considering the similarity to LIB technology.[13,15,16] Although the ideal type of cathode material is still not a consensus since Na_xTMO_2 can undergo some issues that cause low electrochemical performance and structural instability, even so, the aforementioned features place Na_xTMO_2 poised to assume the pivotal role as next-generation cathode materials for SIBs. Therefore, the comprehensive evaluation of the chemical composition, electrochemical performance, structure, and cost of Na_xTMO_2 is fundamental to achieving optimal cathodes for commercial SIBs.[13,15,16]

The several properties of Na_xTMO_2 depend especially on its structure and chemical composition. The chemical composition offers versatility, featuring a wide array of combinations of transition metal ions and alkaline-earth metal ions, including Cr, Fe, Ni, Mn, Co, V, Ti, Zn, Cu, Ru, Sn, Ir, Li, Mg, among others.[13] This versatility brings significant advantages, such as compositional flexibility, increased capacity, and simplified synthesis methods.[13] Moreover, the diverse combinations of transition metals and variations in Na^+ content can result in significant differences in TM–O bond strengths, electronic configurations, and oxidation states, leading to distinct structural differences in the Na_xTMO_2.[13]

During the 1980s, Delmas *et al.*[18] reported the types of stacking arrangements of NaTMOs. Based on layer stacking sequences of oxygen atoms and Na^+ position (coordination) in the structure, Na_xTMO_2 materials can be categorized by O and P types that can be defined as the phases O3, P2, O2, and P3.[4,10,13,14,16–19] O and P represent the Na^+ coordination environment, octahedral and prismatic trigonal, respectively, and the number after the letter (2 and 3) refers to the minimum number of layers of repeated units of oxygen stacked in the structure, *i.e.*, the O-types have Na^+ occupying the octahedral sites between TMO_6 layers, while the P-types have Na^+ occupying the prism sites between TMO_6 layers. Fig. 1a shows the classification of Na_xTMO_2 with TMO_6 layers and the phase transitions induced by sodium extraction. For the O3 type, oxygen atoms are arranged in an "AB CA BC" stacking pattern; for the P2 type, the stacking position of its oxygen atoms follows an "AB BA AB" sequence; for the P3 type, the oxygen atoms are positioned in an "AB BC CA" order; and for the O2 type, the stacking position of oxygen atoms is "AB AC AB".[4,10,13,14,16–19] The thermodynamically stable and predominant crystal architectures of Na_xTMO_2 are primarily the P2-type and O3-type phases.[10,13,16]

P2-type materials exhibit a larger Na layer spacing due to the occupation mode of Na^+ in the triangular prism, where the Na^+ ions are energetically stable and easy to diffuse (Fig. 1b). Such architecture can enhance the transport rate of Na^+ and sustain

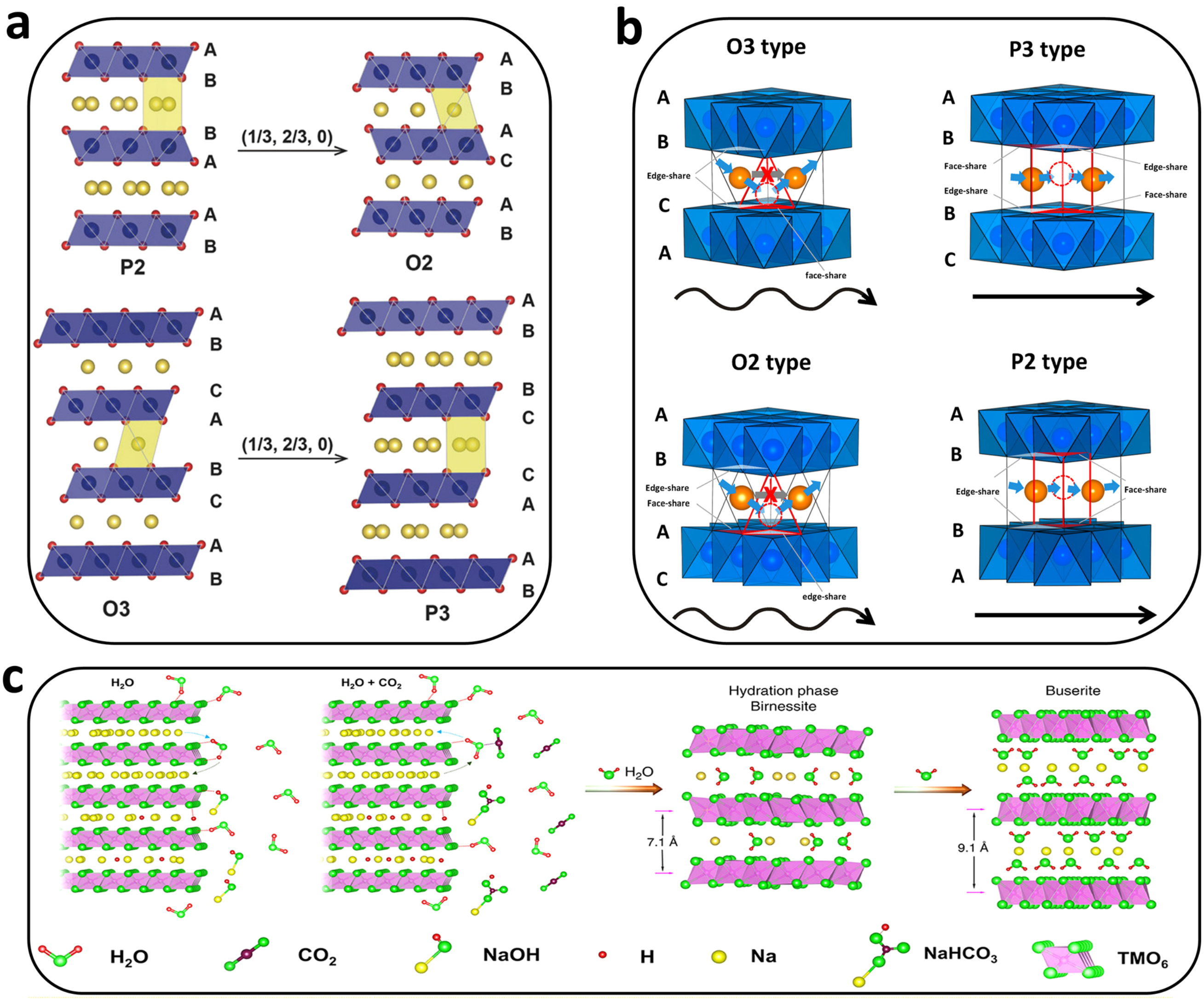

Fig. 1 (a) Structural classification of Na_xTMO_2 with TMO_6 layers and the phase transitions induced by sodium extraction. Reproduced with permission from ref. 20. Copyright © 2017 WILEY-VCH Verlag GmbH & Co. KGaA, Weinheim (b) Na^+ diffusion path in O and P-types of layered transition metal oxides. Reproduced with permission from ref. 19. Copyright © 2014 American Chemical Society. (c) Schematic illustration of processes occurring with Na_xTMO_2 under exposure to air. Reproduced with permission from ref. 15. Copyright © 2023 The Authors. Published by American Chemical Society. This publication is licensed under CC-BY 4.0.

the wholeness of the layered structure, leading to amazing structural stability during charge and discharge processes, improved rate performance, cycling, and air stability.[13] Despite that, their relatively low sodium content ($x \leq 0.7$, Na_xTMO_2) linked to the low initial charge capacity poses challenges for their utilization in high-energy SIBs. In addition, at higher voltages, they undergo an irreversible phase transition from P2 to O2 (Fig. 1a) as sodium ions deintercalate during deep sodium extraction (in the charging and discharging process), which reduces the Na^+ diffusion kinetics, causes volume expansion and structural instability, resulting in compromised rate performance and cycling stability.[10,13,19,20]

On the other hand, O3-phase materials theoretically offer higher specific capacities during charging and discharging owing to their highest Na content ($0.8 \leq x \leq 1.0$, Na_xTMO_2) but possess tortuous Na^+ diffusion channels (Fig. 1b) and relatively unstable structures compared to P2-phase materials.[10,13,19,20] For O3-phase, at higher voltages, multiple and more complex phase transitions occur (O′3, P3, P′3, and P3″), negatively impacting cycling performance.[10,13,19,20] As sodium extraction takes place, the O3-phase develops more prismatic vacancies, forming a thermodynamically stable P3-type phase, as shown in Fig. 1a, which exhibits a relatively lower Na^+ diffusion barrier.[10,13,19,20]

In addition to the mentioned irreversible phase transitions that cause instability in the electrochemical performance during the cycling process, Na_xTMO_2 materials display poor air stability during storage and transportation. External components in the air, such as H_2O, CO_2, and O_2, are harmful to Na_xTMO_2.[16] The molecules of H_2O tend to adsorb on the surface and produce NaOH. CO_2 molecules further aggravate the reaction of H_2O molecules due to their acidity. They can react with water on the surface of Na_xTMO_2 electrodes and produce NaOH, carbonate, and its derivatives, which are electrochemically inert.[4,15,16] After the extraction of a substantial amount of Na^+, water molecules infiltrate into the Na layers, forming hydration phases.[15] A schematic illustration of these processes is shown in Fig. 1c. The mechanism of O_2 molecules has not been completely understood, but it is known that O_2 in the air can oxidize some materials containing low valence metal ions, such as Fe^{2+} and Ti^{3+}.[16]

The issues mentioned here have been the main challenges to be overcome for the production and application of Na_xTMO_2 cathode materials in SIBs. Various strategies, including ion doping, surface coating, structural design/morphology, and those based on the composition and distribution of transition metal ions and sodium content, have been studied in order to solve these issues.[11,16,17,21] Understanding the mechanism and correlation between their structures and electrochemical properties is crucial for the advancement of Na_xTMO_2 cathode materials. Achieving high capacity remains a paramount objective for electrode materials to fulfill the requirements of energy storage devices. Na_xTMO_2 compositions featuring multiple transition metals are increasingly being explored to satisfy the need for cathode materials with enhanced electrochemical performance. Among Na_xTMO_2 materials, Ni-rich NaTMOs have attracted attention. In fact, Ni-based cathodes demonstrate high reversible capacity due to their multi-electron redox reactions and the suitable redox potential of Ni-ions, enabling higher operating voltages.[13,16] In addition, Ni can be utilized as a particulate substitute for other transition metals, resulting in increased specific capacity.[13] Furthermore, Ni-based Na_xTMO_2 materials are qualified as one of the most favorable elements for constructing cathodes for cost-effective and high-energy SIBs, favorable for commercialization.[10,15] Therefore, the development of Ni-rich layered transition metal cathode materials holds significant promise and tangible prospects. Therefore, the subsequent sections of this highlight delve into both main trends and strategies in this hot topic area.

3. Ni-rich layered cathodes in SIBs: general trends

While exploring Ni-rich layered cathodes in Sodium-Ion Batteries (SIBs) is currently in its early stages, there is already potential to delineate future perspectives. This is particularly noteworthy as many of the upcoming stages in this research may echo processes that have previously been undertaken for analogs in LIBs, evoking a sense of "déjà vu". In fact, the industrial feasibility of incorporating Ni-rich layered oxides-based SIB cathodes, due to their similarity to LIB technology and the utilization of established LIB devices, positions layer-structured transition metal oxides as key contenders for next-generation cathode materials in SIBs.[13]

The aforementioned perspectives can be concisely gleaned by analyzing the summarized recent trends presented in Table 1. In fact, as expected, due to their analogous chemistry and widespread use in LIBs, certain compositions are currently under investigation as Ni-rich layered cathodes for SIBs, such as $Na[Ni_xFe_yMn_z]O_2$ (Na-NFM) and $Na[Ni_xCo_yAl_z]O_2$ (Na-NCA) based cathodes. Notably, as a distinctive feature of layered oxide cathodes in SIBs, compositions based on $Na[Ni_xCo_yMn_z]O_2$ (Na-NCM) have been intensely studied, and recent progress shows advances toward Ni-rich Na-NCM. For instance, many compositions based on Na-NCM showed specific capacities greater than 100 mA h g^{-1} even at current densities as high as 5C and 10C.

Conversely, concerning synthesis techniques, a predominant number of Ni-rich NaTMOs have been synthesized *via* the coprecipitation method, followed closely by the utilization of sol–gel methods. While sol–gel and solid-state synthesis methods have their drawbacks, such as the use of expensive precursors, time-consuming processes, and non-uniform particle growth, coprecipitation synthesis emerges as the preferred method for synthesizing scalable and uniform cathodes.[22] In fact, coprecipitation synthesis is a prominent approach for NaTMO fabrication owing to its scalability, capacity to achieve homogeneous distribution of transition metal ions, minimal impurities, and precise control over particle morphology, thereby enhancing electrochemical performance.[23] Particularly for grid-scale energy storage at the commercial scale, considerations of scale-up and engineering aspects are paramount.[23] On the other hand, it is important to note that both coprecipitation and sol–gel methods are used to prepare cathode active material precursors. These methods require additional post-reaction steps to produce the final product. For instance, after the co-precipitation reaction, post-processing techniques such as filtration, precipitate drying, sodiation, and calcination are necessary.[23]

Another noteworthy aspect is the prevalence of the O3-type phase in layered oxide cathode materials for SIBs. Indeed, the structural variance gives rise to discernible differences in the electrochemical characteristics of these layered oxide materials,[13] characterized by a higher Na content, resulting in a higher theoretical specific capacity compared to Na-deficient P2-type oxides.[13,24] Addressing the challenges in developing O3-type layered oxides involves overcoming high Na^+ resistance, limited reversibility at elevated voltages, and structural instability during de-intercalation/intercalation processes,[24,25] along with issues like microcrack formation and cathode-electrolyte interphase on electrode surfaces.[24,26] Subsequent sections will explore strategies and current trends to mitigate these challenges, with a focus on the quest for Ni-rich O3-type layered oxides.

4. Ni-rich $Na[Ni_xCo_yMn_z]O_2$-based cathodes for SIBs

As expected, and even seeming like a déjà vu of what has already been done for LIBs, recent works show the main strategies in the design of Na-NCM with improved mechanical and electrochemical properties. In fact, among the main strategies, materials engineering has been observed through the use of conductive coating materials and the formation of Ni-rich Na-NCM with hierarchical columnar structures, *etc.* Nevertheless, even though cutting-edge research has concentrated on Ni-rich

Table 1 Summary of Ni-rich layered oxides-based cathodes in SIBs[a]

Ni-rich layered oxides	Phase	Strategy or effect	Metals	Synthesis methods	Discharge capacity (mA h g^{-1})	Capacity at high current density rate (mA h g^{-1})	Capacity retention (%)	WVW (V *vs.* Na/Na^+)	Ref.
O3–$NaFe_{0.3}Ni_{0.7}O_2$	O3	—	NiFe	Solid-state	135 @ 30 mA g^{-1}	—	~74 (30 cycles @ 30 mA g^{-1})	2.0–3.8	35
O3–$NaNi_{2/3}Mn_{1/6}Fe_{1/6}O_2$	O3	Lowest Mn^{4+}/Mn^{3+} ratio	NiFeMn	Solid-state	226 @ 0.2C	145 @ 2C	76 (100 cycles @ 0.2C) 70 (138 cycles @ 0.2C)	1.5–4.2	33
O3–$Na[Ni_{0.60}Fe_{0.25}Mn_{0.15}]O_2$	O3	Reasonable upper cut-off voltage		Coprecipitation/calcination	152 @ 0.1C	134 @ 2C	~84 (200 cycles @ 0.5C)	2–4.0	26
$Na[Ni_{0.8}Co_{0.1}Mn_{0.1}]O_2$	O3	The optimal composition	NiCoMn	Coprecipitation/calcination	187.1 @ 15 mA g^{-1}	—	50 (100 cycles @ 75 mA g^{-1})	1.5–4.1	36
$Na_{0.75}Ni_{0.82}Co_{0.12}Mn_{0.06}O_2$	O3	A facile electrochemical ion-exchange strategy		Solid-state	171 @ 1C	89 @ 9C	65 (400 cycles @ 1C)	2.0–4.0	37
$Na[Ni_{0.65}Co_{0.08}Mn_{0.27}]O_2$	O3	Coating + concentration gradient		Coprecipitation/calcination	168 @ 0.5C	—	77 (50 cycles @ 0.5C)	1.5–4.1	30
RAHC $Na[Ni_{0.60}Co_{0.05}Mn_{0.35}]O_2$	O3	Concentration gradient + morphology		Coprecipitation/calcination	~157 @ 0.1C	132.6 @ 10C	84 (100 cycles @ 0.5C)	1.5–4.1	27
$Na[Ni_{0.61}Co_{0.12}Mn_{0.27}]O_2$		Concentration gradient + morphology		Coprecipitation/calcination	160 @ 0.1C	130 @ 10C	80 (100 cycles @ 0.5C)	1.5–4.1	28
AlF_3-coated nanorod gradient $Na[Ni_{0.65}Co_{0.08}Mn_{0.27}]O_2$	O3	Coating + concentration gradient	NiCoMn + material-coated	Coprecipitation/dry ball-mill coating	161 @ 0.5C	145 @ 5C	90 (50 cycles @ 1C)	1.5–4.1	30
Al_2O_3 coated Na $[Ni_{0.6}Co_{0.2}Mn_{0.2}]O_2$	O3	Coating		Coprecipitation/dry ball-mill coating	151 @ 0.1C	115 @ 10C	91 (50 cycles @ 0.5C)	1.5–4.1	29
O3–Na $[Ti_{0.03}(Ni_{0.6}Co_{0.2}Mn_{0.2})_{0.97}]O_2$	O3	Doping	NiCoMn–Ti	Solid-state	154 @ 0.1C	~108 @ 10C	87 (100 cycles @ 0.5C)	1.5–4.1	31
$NaNi_{0.6}Co_{0.2}Mn_{0.2}O_2$T-CSN6@A	O3	Core–shell design + doping + surface coating	NiCoMn–Ti + material-coated	Coprecipitation/calcination	163.5 @ 0.1C	118.5 @ 10C	85.4 (200 cycles @ 0.5C)	1.5–4.1	38
$NaNi_{0.8}Co_{0.15}Al_{0.05}O_2$ (quenched O3)	O3	Materials engineering: phase study	NiCoAl	Solid-state	162 @ 0.1C	—	~90 (120 cycles @ 0.1C)	1.5–3.9	32
$NaNi_{0.8}Co_{0.15}Al_{0.05}O_2$ (slow-cooled O′3)	O′3	Materials engineering: phase study		Solid-state	150 @ 0.1C	—	~90 (120 cycles @ 0.1C)	1.5–3.9	32
$NaNi_{0.8}Co_{0.15}Al_{0.05}O_2$	O′3	Monoclinic phase		Coprecipitation/calcination	153.9 @ 0.1C	91.5 @ 5C	93.2 (100 cycles @ 1C) 86.7 (200 cycles @ 1C)	2.0–3.8	1

[a] RAHC = Radially aligned hierarchical columnar structure.

compositions for LIB cathodes, the development in the realm of SIBs is still in its early phases.[24]

Taking into account the encouraging outcomes outlined in Table 1, the utilization of concentration gradient materials proves advantageous for achieving remarkable electrochemical properties and ensuring excellent safety in battery systems.[27] This is attributable to the compact rod assembly, effectively minimizing the surface area in contact with the electrolyte.[27] Consequently, this design mitigates the exposure of active materials to the acidic electrolyte, providing protection against hydrogen fluoride (HF) attack.[27] Adopting a comparable approach, Hwang *et al.*[27] designed a radially aligned hierarchical columnar structure within spherical particles, featuring a varied chemical composition ranging from the inner end ($Na[Ni_{0.75}Co_{0.02}Mn_{0.23}]O_2$) to the outer end ($Na[Ni_{0.58}Co_{0.06}Mn_{0.36}]O_2$) of the structure (Fig. 2a). The determined average chemical composition of the resulting Na-NCM was identified as $Na[Ni_{0.60}Co_{0.05}Mn_{0.35}]O_2$ (Na-NCM60). This architectural design leads to decreased electrochemical and thermal decomposition of the active material. Furthermore, the radially aligned long columnar structure proves advantageous in minimizing contact with the electrolyte (Fig. 2b and c). Consequently, this design exhibits remarkably high capacity in a Na system, showcasing approximately 157 mA h g^{-1}, along with an impressive capacity retention of 84% over 100 cycles due to the noteworthy $Ni^{2+/3+/4+}$ redox reaction. Implementing this approach yielded higher capacity retention compared to traditional bulk cathode materials and numerous other pristine Na-NCM variants (refer to Table 1).

Motivated by their earlier achievements, the same research group has detailed a new synthesis technique that generates Na ion insertion cathode materials.[28] To delve into specifics, the researchers engineered spoke-like nanorod assemblies (SNAs) organized within spherical secondary particles. This design aimed to enhance both electrochemical and physicochemical properties by modulating the chemical composition from the inner end ($Na[Ni_{0.75}Co_{0.08}Mn_{0.17}]O_2$) to the outer end ($Na[Ni_{0.58}Co_{0.14}Mn_{0.28}]O_2$) (Fig. 2d–i). The resulting cathode material exhibits an average composition of $Na[Ni_{0.61}Co_{0.12}Mn_{0.27}]O_2$ (Na-NCM61). As per the authors, modifying the chemical composition of these sodiated Na-NCMs can substantially alter their mechanical properties, integrity, and stability. The deliberate increase in the Co content (11% in the new SNAs, as opposed to 5% in RAHCs) is aimed at enhancing their electrochemical properties, specifically focusing on improving the initial coulombic efficiency and rate capability. Moreover, they employed an enhanced synthesis method for the SNA Na-NCM61 cathode material, utilizing a batch reactor as opposed to the continuously stirred tank reactor used for RAHC Na-NCM60. The cathode materials synthesized through the batch reactor exhibited a narrow particle size distribution, increased concentration homogeneity, more densely packed particle characteristics, and outstanding mechanical properties, which exhibit a strong correlation with their excellent electrochemical performances. In fact, the mechanical strength of the spherical particles composed of SNAs surpasses that of particles containing Na-NCM61 moieties with constant concentration (CC). These structural and morphological characteristics contribute to achieving high discharge capacities, with values of 160 mA h g^{-1} at 0.1C. Furthermore, the SNA Na-NCM61 cathode demonstrates superior capacity retention compared to the CC cathode, recording approximately 80% *versus* 63.4% after 100 cycles (Fig. 2j and k), which can be attributed to the better-integrated structure and enhanced mechanical strength of the SNA Na-NCM61 cathode. Notably, the SNA Na-NCM61 cathode exhibits remarkable capacity retention, reaching 98% at −20 °C after 100 cycles, corresponding to a discharge capacity of 107 mA h g^{-1}. These studies represent a notable leap forward in the advancement of novel cathodes for sodium-ion insertion with a concentration gradient.

Conversely, another widely employed approach in LIBs, and one that is emerging in the realm of SIBs, involves advancing coating materials to efficiently reduce undesirable reactions with the electrolyte solution while simultaneously aiding the migration of Na^+ ions. Thus, to address the heightened capacity fade linked to increased Ni content, driven by the pronounced reactivity of Ni^{4+} with the electrolyte, a surface modification strategy has been implemented. This approach aims to augment the cyclic stability of some Ni-rich Na-NCM-based cathodes. A notable illustration of this methodology was presented by Hwang and colleagues.[29] In their research, they employed a straightforward dry ball-milling process to surface-modify an O3-type Na-NCM60 cathode, incorporating Al_2O_3 nanoparticles (Fig. 3a). These nanoscale Al_2O_3 particles, measuring approximately 15 nm in diameter, effectively encased the spherical O3-type Na-NCM60 cathode particles (Fig. 3b–d). This coating mitigated undesired reactions with the electrolyte and facilitated the migration of Na^+ ions. The resultant Al_2O_3-coated Na-NCM60 cathode exhibited a specific capacity of 151 mA h g^{-1}, coupled with enhanced cycling stability of 91% after 50 cycles at 0.5C (Fig. 3e), along with notable rate capability (Fig. 3f). In summary, the utilization of nanomaterial coating strategy plays a pivotal role in protecting against HF attack and preventing Ni^{4+} oxidation reactions. These compounds, positioned near the surface of the electrode material, play a crucial role in stabilizing interface chemistry and reducing charge transfer resistance, effectively counteracting cathode degradation.[29] This phenomenon facilitates Na^+ conductivity,[29] thereby significantly improving electrochemical performance, as highlighted in the cited literature.

Remarkably, our recent research has revealed that the combination of various strategies has yielded even more promising results within the realm of LIBs. Naturally, analogous directional trends have been observed for the same approach in SIBs. In fact, many Ni-rich electrode materials with capacity retention greater than 80% (after 50 or more cycles) incorporated in Table 1 report the use of more than one strategy to mitigate the low mechanical and thermal stability of these systems. In this scenario, Sun *et al.*[30] employed a synergistic approach involving the strategic design of a radially nano-columnar composition gradient and the application of dry ball-mill coating. This innovative technique aims to yield a cathode with both a remarkably high capacity and a consistently stable cycling performance for a nanorod gradient Ni-rich O3-type Na-

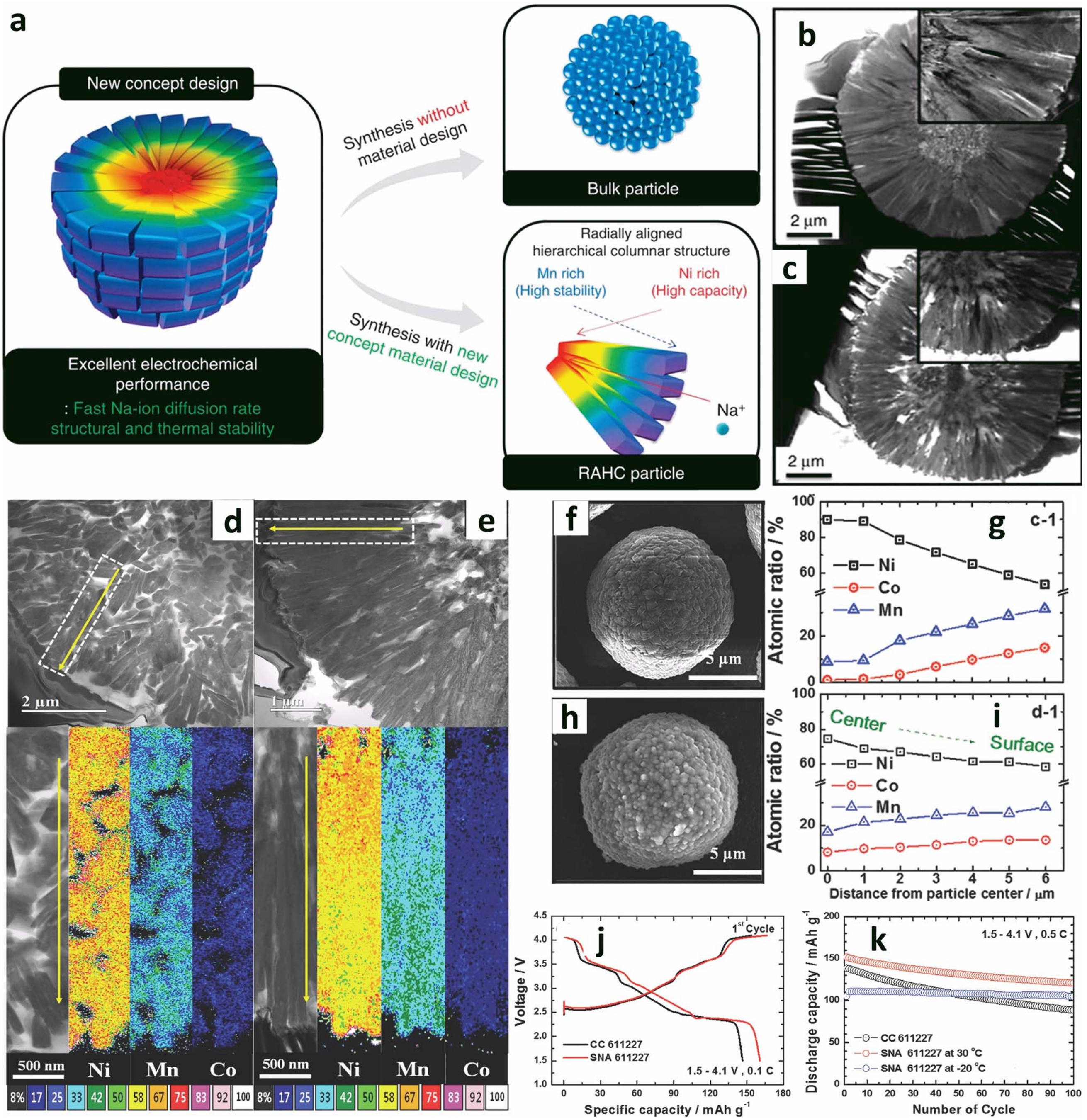

Fig. 2 (a) (Left) Representative hemisphere image showcasing the innovative cathode material concept design. (Right) (Top) Depiction of a single particle of traditional bulk cathode materials; (Bottom) Illustration of the microstructure featuring a radially aligned hierarchical columnar structure, indicative of the developed cathode materials with the novel concept design. (b) Cross-sectional TEM image of (b) RAHC [$Ni_{0.60}Co_{0.05}Mn_{0.35}](OH)_2$ and (c) sodiated Na-NCM60. Adapted with permission from ref. 27. Copyright © 2015, Springer Nature Limited. Cross-sectional TEM images and the corresponding EDAX mapping (in a selected rectangular area) are presented for (d) a representative CC Na-NCM61 particle and (e) an SNA Na-NCM61 particle. (f) An SEM image capturing a particle of the precursor SNA $Ni_{0.61}Co_{0.12}Mn_{0.27}(OH)_2$, while (h) presents an image of an SNA Na-NCM61 particle post-sodiation and quenching. The 2D electron probe microanalyzer reveals results for (g) the SNA $Ni_{0.61}Co_{0.12}Mn_{0.27}(OH)_2$ particle and (i) the SNA Na-NCM61 particle after sodiation and thermal quenching. (j) The voltage profiles for the initial charge and discharge are illustrated at a 0.1C rate. (k) The capacity retention over 100 cycles is depicted at 0.5C. Reproduced with permission from ref. 28. Copyright © 2016 WILEY-VCH Verlag GmbH & Co. KGaA, Weinheim.

NCM65 composition (Fig. 3g and h). In more detail, the nanorod gradient Na-NCM65 (named NRG65) particle is structured with a Ni-rich core to ensure high capacity, while its Mn-rich surface enhances cycling stability. This design results in superior electrochemical performance when compared to the conventional Na-NCM65 with a constant concentration (Fig. 3i and j). Besides, as per the authors, the efficacy of a protective AlF_3 coating surpasses that of Al_2O_3 coatings. This

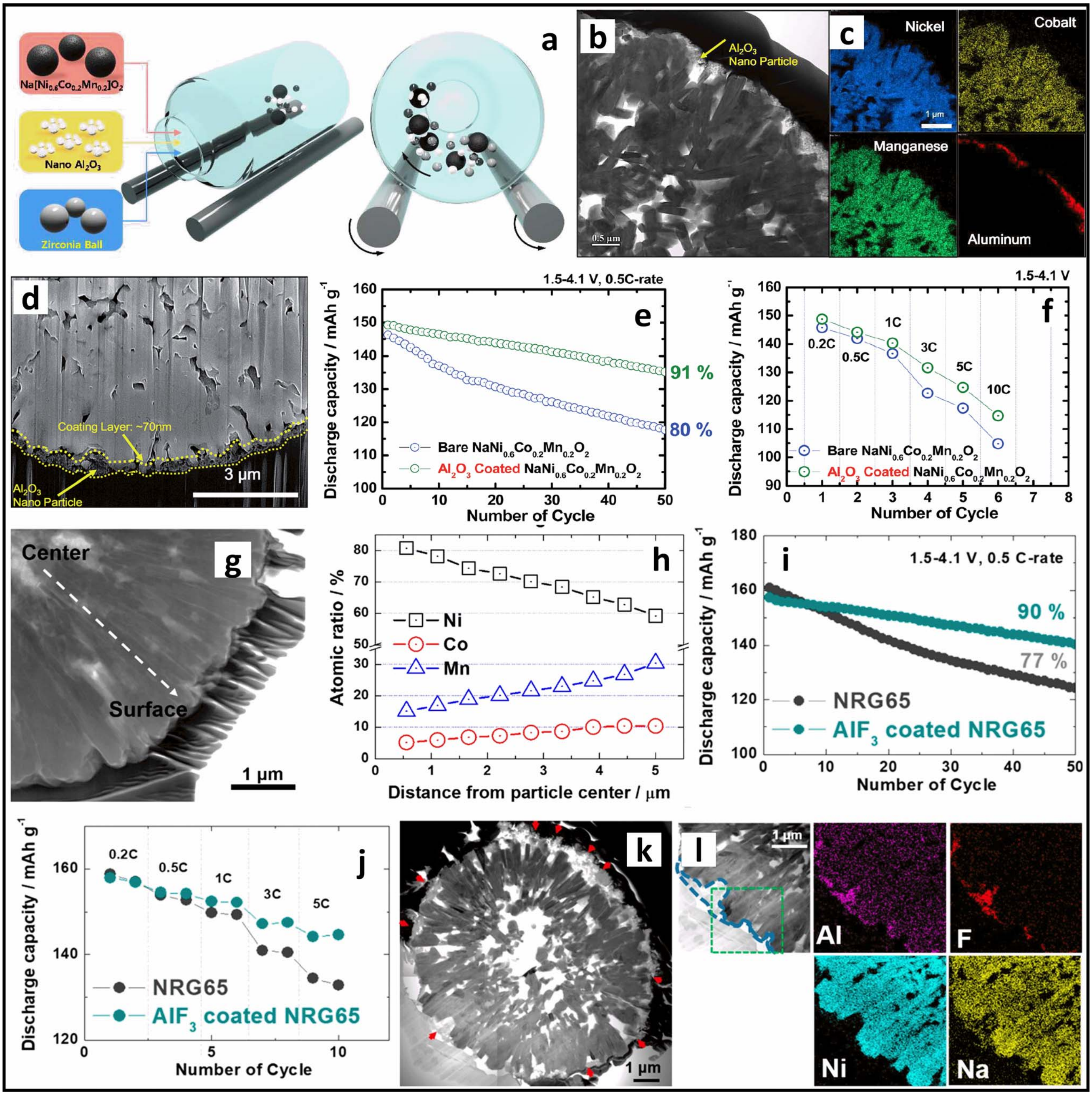

Fig. 3 (a) A schematic representation of the ball-mill coating process employed in the production of an Al_2O_3-coated Na-NCM60 cathode. (b) Cross-sectional TEM image and (c) EDS-TEM mapping of Al_2O_3-coated Na-NCM60 particle. (e) Capacity retention at a 0.5C and (f) rate capability test of the bare Na-NCM60 and Al_2O_3-coated Na-NCM60 cathode Reproduced with permission from ref. 29. Copyright © The Royal Society of Chemistry. (g) Cross-sectioned TEM image and (h) electron probe microanalyzer data showcasing the as-synthesized nanorod gradient Na-NCM65. (i) Cycling and (j) rate performance of bare NRG65 and AlF_3-coated NRG65. (k) Bright-field scanning TEM cross-sectional image depicting the cycled AlF_3-NRG65 cathode particle after 200 cycles, with red arrows highlighting the intact AlF_3 coating post-cycling. (l) EDS elemental mapping of the cycled AlF_3-NRG65 cathode particle. Reproduced with permission from ref. 30. Copyright © 2018 American Chemical Society.

enhancement is attributed to its ability to impede electrolyte side reactions and decomposition, thereby retarding the dissolution of active materials. Additionally, AlF_3 stands out as a more stable alternative when contrasted with Al_2O_3, owing to its lower Gibbs free energy of formation and stability up to 4.5 V. Furthermore, fluoride-based compounds, in general, exhibit greater resistance to moisture in ambient air compared to their oxide counterparts (Fig. 3k and l). Consequently, the cathode material comprising NRG65 demonstrates remarkable performance attributes, showcasing a substantial discharge capacity of 160 mA h g^{-1}, exceptional capacity retention at 89.2%, and a promising rate capability, as illustrated in Fig. 3i and j.[30]

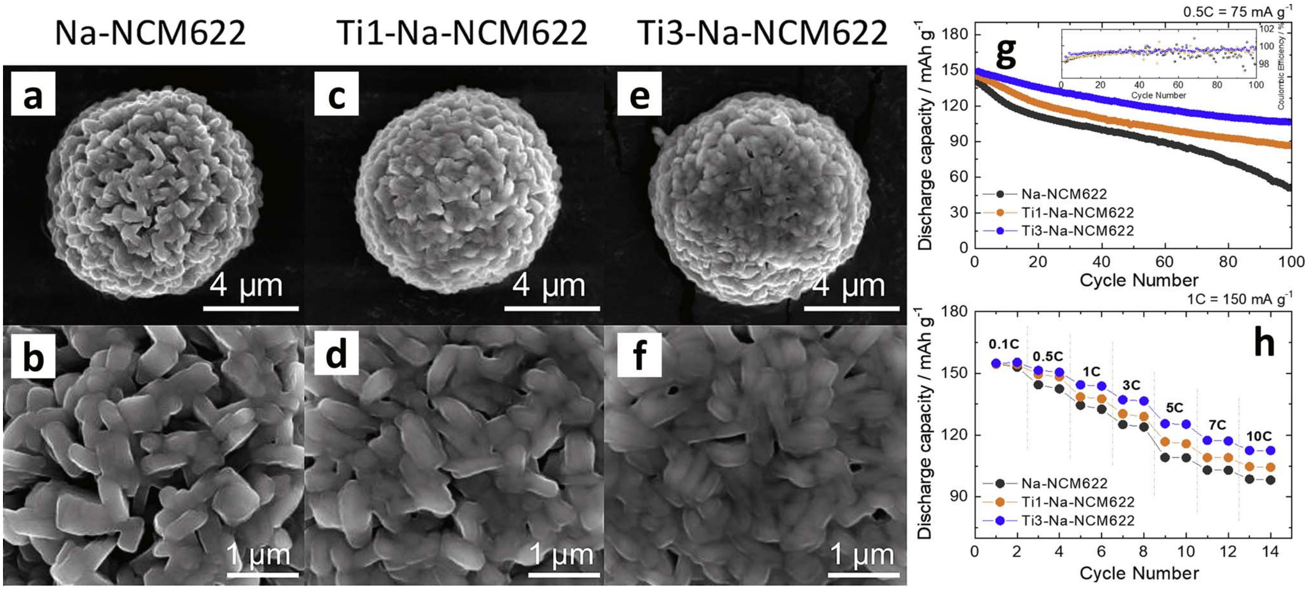

Fig. 4 SEM images of (a and b) undoped and (c–f) Ti-doped Na-NCM622. (b) Cycling performance at 75 mA g^{-1}, with inset images depicting coulombic efficiency *versus* cycling number. (c) Rate capability tests were conducted at various current densities ranging from 15 mA g^{-1} to 1500 mA g^{-1}. Reproduced with permission from ref. 31. Copyright © 2019 Elsevier B.V. All rights reserved.

It is crucial to emphasize that, unlike the extensively documented advancements in LIBs, the comprehensive exploration of incorporating a fourth or more metals *via* a doping strategy remains largely unexplored in Ni-rich cathodes for SIB electrodes. While further in-depth exploration is required, integrating inactive elements into the design of multielement Ni-rich cathodes may emerge as a promising strategy for developing electrodes with significant capacity and outstanding cycling stability by inhibiting phase transitions. Notably, among the inactive ions warranting exploration, Ti^{4+} and Mg^{2+} stand out.[24] This underscores the pivotal role inactive elements can play in stabilizing the structure during Na^+ migration.[24] In this context, Yu and colleagues[31] investigated the impact of partial Ti doping on the structural and electrochemical properties of O3-type Ni-rich Na-NCM6222 materials. They varied the Ti content from 0 to 0.03 SEM images revealed that upon doping, the primary particles aggregated to form densely packed secondary particles, resulting in enhanced mechanical strength and high tap density (Fig. 4a–f). This compact particle morphology effectively reduced void volume, thereby minimizing electrolyte penetration and associated undesirable side reactions. Furthermore, partial Ti doping in the transition-metal layer significantly improved structural stability. Leveraging both morphological and structural advantages, the O3-type $Na[Ti_{0.03}(Ni_{0.6}Co_{0.2}Mn_{0.2})_{0.97}]O_2$ cathode exhibited remarkable enhancements in battery performance, including increased capacity, cycle retention (Fig. 4g), rate capability (Fig. 4g), and improved thermal properties. These findings suggest a promising avenue for designing and developing transition metal oxide cathodes for high-performance sodium-ion batteries.

5. Ni-rich $Na[Ni_xCo_yAl_z]O_2$-based cathodes for SIBs

A subgroup of Ni-rich $Na[Ni_xCo_yAl_z]O_2$ (Na-NCA) layered oxides, akin to the notable advancements in LIBs, that has garnered

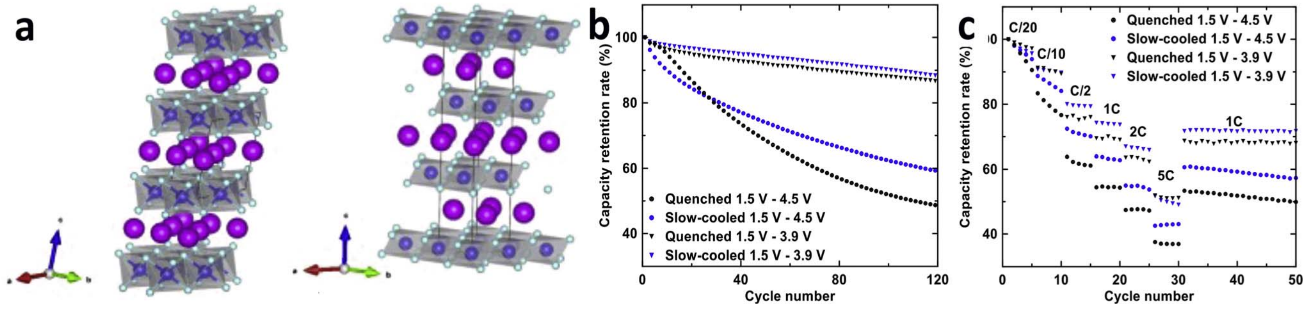

Fig. 5 (a) Schematic representation of the structure of hexagonal O3 and monoclinic O′3 layered-type oxides. Comparison of the (b) cycling performance and (b) rate performance between O3 Na-NCA and O′3 Na-NCA. Reproduced with permission from ref. 32. Copyright © 2019 Elsevier B.V. All rights reserved.

attention for SIB applications are cathodes based on Na-NCA. Indeed, for all three compositions listed in Table 1, the capacity retention exceeds 90% even after 100 or more cycles. In fact, much like their lithium-ion counterparts, Na-NCA cathodes aim to strike a balance between high capacity, cycling stability, and safety. Besides, drawing an analogy with LIBs, the incorporation of aluminum through doping enhances stability and safety, attributed to the strong Al–O bond.[32] In addition, substituting a portion of nickel with cobalt enhances electrochemical performance.[32] Consequently, $LiNi_xCo_yAl_zO_2$ (NCA) materials have undergone a thorough investigation and are widely adopted in commercial LIBs.[32]

On the other hand, despite limited research on the advancement of Ni-rich Na-NCA, there is potential for significant future progress. This potential stems from the ability to design Na-NCA with varying phases, indicating promising avenues for further exploration and development in the field. For instance, Zheng *et al.*[32] successfully designed Na-NCA80 materials with hexagonal O3 or monoclinic O′3 structures (Fig. 5a). These structures were synthesized for the first time using either quenching or slow-cooling methods applied to heated precursors. The structural differences observed between the quenched O3-type and slow-cooled O′3-type Na-NCA80 materials were attributed to the presence of oxygen vacancies during the cooling process. Both materials demonstrated superior electrochemical performance compared to $NaNiO_2$. Moreover, it was determined that O′3 Na-NCA exhibits superior cycling performance due to its inherently more stable structure at room temperature. Notably, when cycled within the voltage range of 1.5–3.9 V, both materials display commendable capacity retention, retaining approximately 90% of their capacity after 120 cycles. However, when subjected to a wider voltage range of 1.5–4.5 V, both materials demonstrate capacity fade, albeit O′3 Na-NCA shows a slightly better performance compared to O3 Na-NCA (Fig. 5b). Additionally, O′3 Na-NCA displays notably enhanced rate capability compared to O3 Na-NCA across all cycling voltage ranges (Fig. 5c). Specifically, when cycled within the range of 1.5–3.9 V, O′3 Na-NCA retains 80%, 75%, and 65% of its capacity at C/2, 1C, and 2C current rates, respectively, while O3 Na-NCA retains 75%, 70%, and 60%, respectively. This improved performance of O′3-NCA over O3-NCA can be attributed to its more stable structure at room temperature, as evidenced by the gradual transition of O3-NCA to O′3-NCA during cycling.

Notably, other research also underscores the promising performance of Ni-rich O′3-type layered Na-NCA exhibiting a monoclinic phase structure for SIBs.[1] In fact, the monoclinic Na-NCA80 microspheres demonstrate an initial reversible capacity of 153.9 mA h g^{-1} with a coulombic efficiency of 89.1% at 0.1C. Remarkably, the electrode exhibits a retention capacity of 86.7% after 200 cycles at 1C, indicating its potential as a high-capacity and stable cathode material for SIB applications. According to the authors, the substitution of ions with similar ionic radii and the same valence, such as Co^{3+} and Al^{3+} for Ni^{3+}, enhances the structural stability and improves the reversibility of phase transitions during (de)sodiation processes. Moreover, the hierarchical architecture of the microspheres, along with the assembly of primary nanocrystals, enables high compacted density and offers short diffusion paths for sodium ion/electron transport simultaneously.[1]

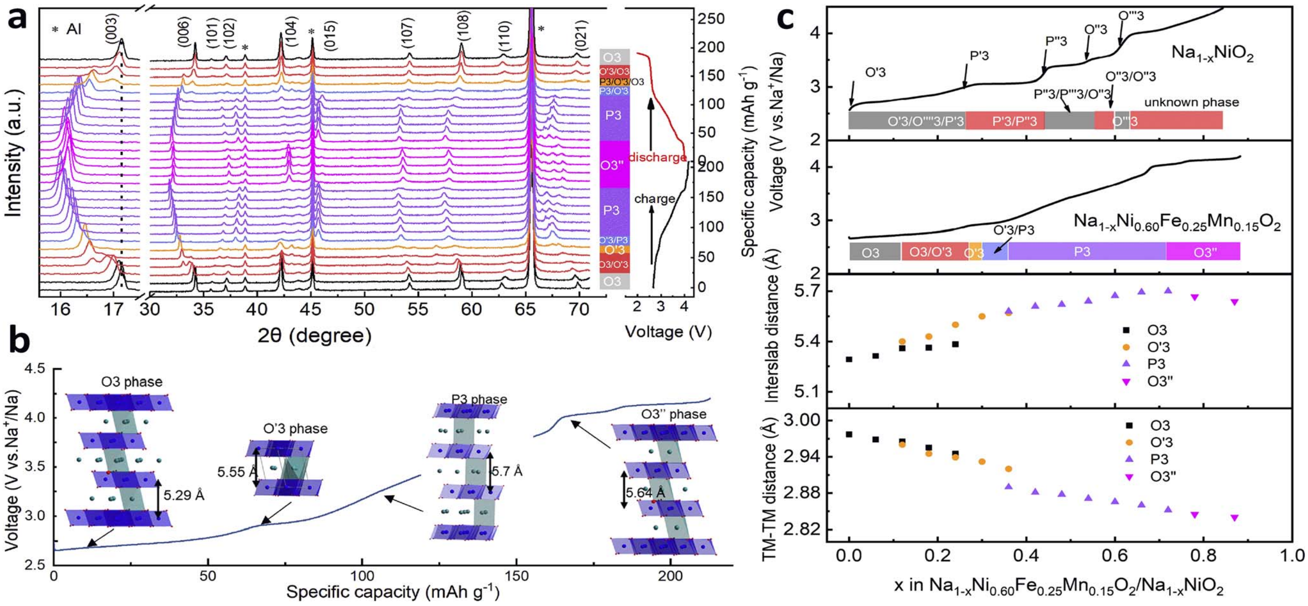

Fig. 6 Structural evolution during charge/discharge is depicted as follows: (a) *in situ* XRD patterns obtained during the initial cycle at 0.1C within the voltage range of 2.0–4.2 V for $Na_{1-x}Ni_{0.60}Fe_{0.25}Mn_{0.15}O_2$ in a sodium half-cell. The corresponding phases and voltage–capacity profile are provided on the right side. (b) The corresponding crystal structure evolution of O3-NNFM at various charged states is illustrated. (c) The variation in transition metal-transition metal (TM–TM) and interslab distances is analyzed as a function of sodium concentration, along with the phase transformation observed in the $Na_{1-x}Ni_{0.60}Fe_{0.25}Mn_{0.15}O_2$ system during the charging process. For comparison, the phase evolution of the $Na_{1-x}NiO_2$ cathode is depicted at the top. Reproduced with permission from ref. 26. Copyright © 2023 Elsevier B.V. All rights reserved.

It's noteworthy to emphasize that the utilization of monoclinic O′3 layered-type oxides in the context of Ni-rich Na-NCA for SIBs holds significant promise. The prospect of future advancements and the necessity for further research in this domain echo a sense of déjà vu akin to the trajectory previously observed in LIBs.

6. Ni-rich Na[$Ni_xFe_yMn_z$]O_2-based cathodes for SIBs

In our recent and comprehensive review,[24] we have noted significant advancements in the design of Na[$Ni_xFe_yMn_z$]O_2 (Na-NFM), mainly focusing on compositions near equimolar concentration, specifically within the realm of medium-entropy Na-NFM. Notably, the substitution of Co^{3+} for Fe^{3+} not only lowers the cost of Na-NFM analog cathode material but also boosts the specific capacity.[33] In fact, cathodes comprising sodium-containing Fe–Mn-based compounds show promise for practical SIBs owing to their abundance of raw materials, low cost, and potential for high electrochemical performance.[34]

Following the same trend and strategies as Ni-rich Na-NCM cathodes, Table 1 also reveals that the design of Ni-rich O3-type Na-NFM layered oxides has been reasonably well reported. However, it is essential to acknowledge that these materials commonly encounter structural impairment in the highly desodiated state.[24,26] In fact, Ding *et al.*[26] identified several reasons for the decay in high-voltage capacity. They reported that the thermodynamic instability of the high-voltage phase is attributed to reduced Na^+ content in the crystal structure. Additionally, significant volume changes during the evolution of the high-voltage phase lead to slower Na^+ diffusion kinetics. Moreover, the study highlights the formation of microcracks and the cathode-electrolyte interphase on the surface of cathode particles as contributing factors.

To address the challenges linked to O3-type Ni-rich Na-NFM, various strategies can be explored, as previously reported for other Ni-rich layered oxides. In that regard, Ding *et al.*[26] reported a reasonable upper cut-off voltage of 4.0 V that was set as a strategy to mitigate the formation of the O3″ phase and minimize electrolyte decomposition. In this investigation,

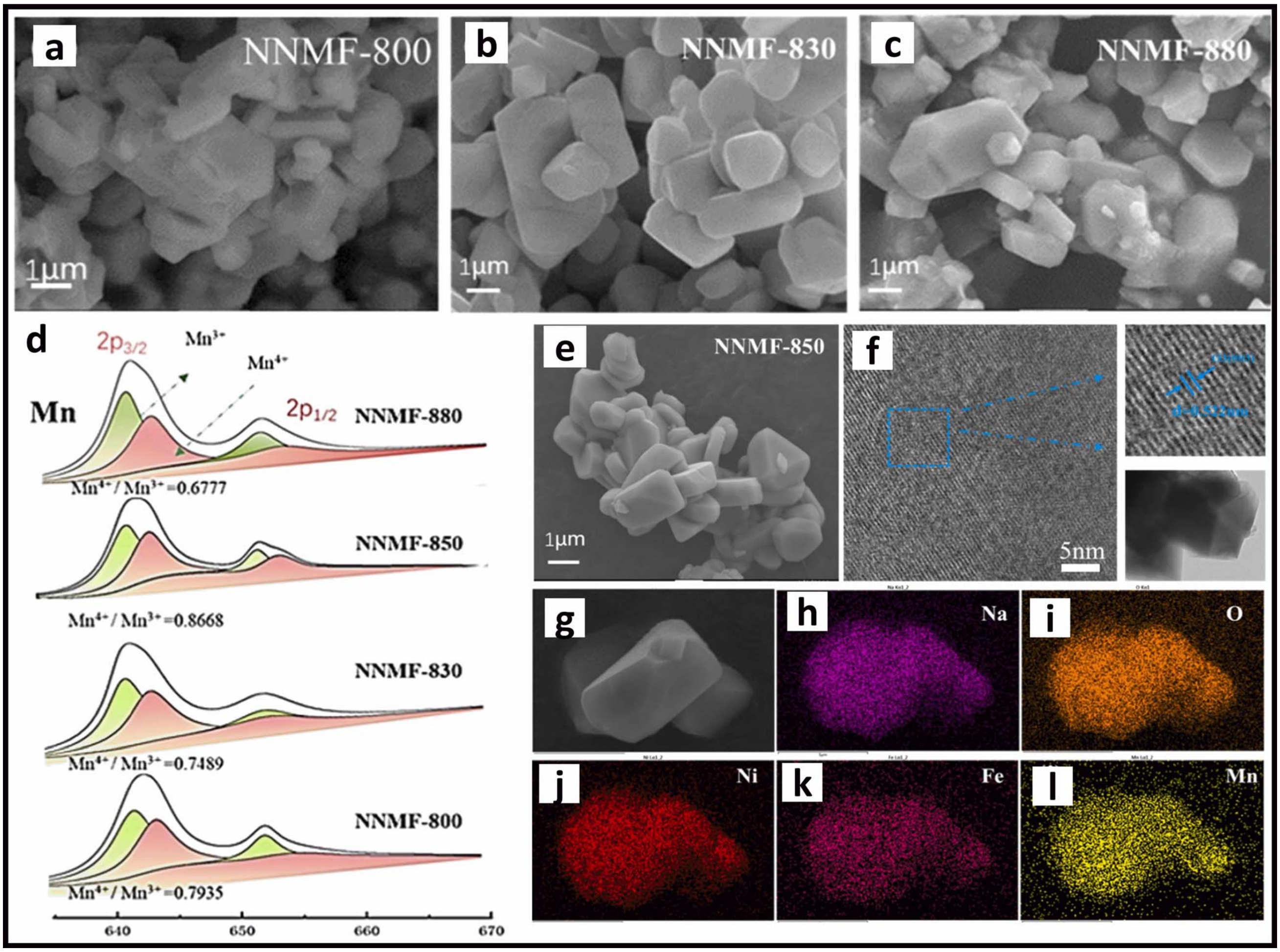

Fig. 7 SEM images of (a) NNMF-800, (b) NNMF-830, (c) NNMF-880. (d) XPS spectra comparison of Mn $2p_{2/3}$ for NNMF-800, NNMF-830, NNMF-850, and NNMF-880 samples. (d) SEM images of NNMF-850. Elemental distribution mapping of Na, Ni, Fe, Mn, and O in NNMF-850 is depicted in panels (g–l). Additionally, a TEM image of NNMF-850 is shown in panel (f). Reproduced with permission from ref. 33. Copyright © 2023 Elsevier B.V. All rights reserved.

a series of Ni-rich oxide cathodes, labeled as O3–Na[Ni_xFe_y-Mn_{1-x-y}]O_2 (with $x = 0.6$, 0.7, and 0.8), were specifically designed. These were denoted as O3-NNFM, O3-NNFM1, and O3-NNFM2, respectively. As expected for a material with a reduced nickel concentration, the O3-NNFM material exhibits superior capacity retention during extended cycling. It retains over 80% of its initial capacity after 100 cycles in the voltage range of 2.0–4.2 V at 0.2C, contrasting with approximately 70% and 63% capacity retention observed for the O3-NNFM1 and O3-NNFM2 samples, respectively. This difference may stem from the higher content of Fe–Mn in the lattice framework of O3-NNFM, which likely enhances structural stability significantly. In fact, in comparison to $NaNiO_2$, the presence of Fe^{3+} and Mn^{4+} within the structure exerts a stabilizing effect, leading to a notable reduction in the occurrence of structural changes. Interestingly, by reducing the charge cut-off voltage to 4.0 V, a comprehensive improvement in performance was achieved for O3-NNFM due to the absence of the high-voltage phase. This resulted in an approximately 84% capacity retention after 200 cycles at 0.5C. A combination of *ex situ* X-ray Absorption Spectroscopy (XAS) and *in situ* X-ray Diffraction (XRD, Fig. 6a–c) analyses was conducted to investigate the reaction mechanism. It was revealed that nickel and iron cations primarily participate in the charge compensation mechanism, accompanied by a highly reversible O3–O′3-P3-O3″ phase transition upon Na^+ (de)intercalation. Notably, the high-voltage O3″ phase exhibited inferior Na^+ diffusion kinetics and thermodynamic stability. Thus, reducing the charge voltage from 4.2 to 4.0 V effectively eliminated the high-voltage O3″ phase, leading to excellent comprehensive performance of the electrode.

As previously noted in the aforementioned study, the presence of Mn^{4+} ions in the Ni-rich Na-NFM cathode is significant, particularly for enhancing capacity retention over extended cycling periods. Following this trend, research conducted by Li *et al.*[33] revealed that the synthesis temperature of electrode materials was raised from 800 °C to 880 °C (Fig. 7a–c). This increase from 800 °C to 850 °C facilitates the formation of Mn^{4+} oxidation states by suppressing the Jahn–Teller effect associated with Mn^{3+} and reducing lattice strain and phase transitions related to Na^+/vacancy ordering. As the temperature rises, NNMF-850 demonstrates the highest Mn^{4+}/Mn^{3+} ratio of 0.8668, whereas NNMF-880 exhibits the lowest ratio at 0.6777 (Fig. 7d). This results in the formation of more stable structures characterized by lower sodium concentration, contributing to a higher reversible capacity. These Ni-rich Na-NFM cathodes displayed a remarkable initial discharge capacity of 226 mA h g^{-1} at a rate of 0.2C.[33] Considering the promising results obtained in the study by Li and colleagues,[33] which demonstrated the significant impact of temperature on the formation of Mn^{4+} oxidation states and the resulting electrochemical performance of Ni-rich Na-NFM cathodes, future research could focus on further optimizing the synthesis conditions to maximize the Mn^{4+}/Mn^{3+} ratio.

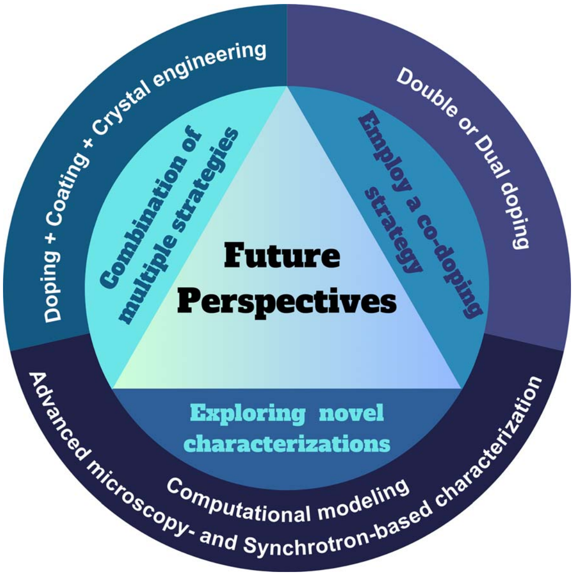

Scheme 2 A schematic illustration depicting possible research directions and significant opportunities that deserve continuous attention for the next generation of Ni-rich cathode materials for SIBs.

7. Conclusions and prospects

In conclusion, while the exploration of Ni-rich layered cathodes in Sodium-Ion Batteries (SIBs) is still in its nascent stages, there are already significant potential future perspectives to consider. This is particularly noteworthy given that many forthcoming stages in this research may mirror processes previously undertaken for analogs in Lithium-Ion Batteries (LIBs), invoking a sense of “déjà vu”. Indeed, the industrial feasibility of incorporating Ni-rich layered oxides-based SIB cathodes, owing to their similarity to LIB technology and the utilization of established LIB devices, positions layer-structured transition metal oxides as key contenders for next-generation cathode materials in SIBs.

These perspectives are succinctly illuminated by analyzing the recent trends summarized in Table 1. As anticipated, certain compositions, such as Na[$Ni_xFe_yMn_z$]O_2 (Na-NFM) and Na[Ni_x-Co_yAl_z]O_2 (Na-NCA) based cathodes, are currently under investigation as Ni-rich layered cathodes for SIBs. Notably, compositions based on Na[$Ni_xCo_yMn_z$]O_2 (Na-NCM) have been intensely studied as a distinctive feature of layered oxide cathodes in SIBs, with recent progress showing advancements towards Ni-rich Na-NCM.

Recent works have highlighted the main strategies in the design of Na-NCM with improved mechanical and electrochemical properties, resembling processes undertaken for analogs in LIBs. Strategies such as materials engineering through the use of conductive coating materials and the formation of Ni-rich Na-NCM with hierarchical columnar structures have shown promise. In fact, the synergistic design of nanocolumnar composition gradients and the application of coating have yielded cathodes with high capacity and stable cycling performance. Furthermore, exploring the incorporation of inactive elements into Ni-rich cathodes *via* a doping strategy holds promise for developing electrodes with significant capacity and outstanding cycling stability by inhibiting phase transitions. Partial Ti doping, for example, has shown enhanced battery performance, including increased capacity, cycle retention, rate capability, and improved thermal properties.

For the Na[Ni$_x$Co$_y$Al$_z$]O$_2$ (Na-NCA) subgroup, Ni-rich Na-NCA cathodes demonstrate impressive capacity retention exceeding 90% even after extended cycling, emphasizing their potential for high capacity, cycling stability, and safety. The incorporation of aluminum through doping enhances stability and safety while substituting nickel with cobalt enhances electrochemical performance, similar to the strategies employed in LIBs. Structural differences observed between different phases, such as hexagonal O3 and monoclinic O′3 structures, impact electrochemical performance, with the latter exhibiting superior stability and rate capability. This underscores the importance of phase engineering in optimizing cathode materials for SIBs.

On the other hand, the substitution of Co^{3+} for Fe^{3+} not only reduces the cost of Na-NFM cathode materials but also enhances specific capacity. As a result, the design of Ni-rich O3-type Na-NFM layered oxides has been reasonably well reported, although these materials commonly encounter structural impairment at the highly desodiated state. Thus, to address the challenges linked to O3-type Ni-rich Na-NFM, various strategies can be explored, such as setting a reasonable upper cut-off voltage to mitigate the formation of the O3″ phase and minimize electrolyte decomposition. Besides, the higher content of Fe–Mn in Ni-rich Na-NFM layered oxides enhances structural stability significantly. In fact, raising the synthesis temperature of electrode materials facilitates the formation of Mn^{4+} oxidation states, resulting in more stable structures with higher reversible capacity.

Although research on Ni-rich layered oxide cathodes is limited, there is significant potential for future progress. Recent studies have successfully designed Ni-rich layered oxide materials, indicating promising avenues for further exploration and development. Nevertheless, several challenges and bottlenecks must be addressed to achieve the mass production, practical application, and commercialization of the next generation of Ni-rich layered oxides for SIBs. To overcome these significant limitations, the following future perspectives and directions could be implemented, as summarized in Scheme 2 and highlighted below:

(i) Recent studies in the realm of LIBs have demonstrated the effectiveness of combining multiple strategies, such as doping (single or dual doping), coating, and crystal engineering, to suppress phase transitions and mitigate chemical and mechanical degradation. In this regard, future research should continue along similar lines, combining strategies such as doping with coating, crystal engineering with coating, and others. These approaches hold the potential to yield superior capacity retention even after hundreds of charge–discharge cycles.

(ii) Research into the design of Ni-rich cathodes doped with two or more metal ions remains relatively scarce. In this context, employing a co-doping strategy (double or dual doping) for Na-NCMs, Na-NCAs, or Na-NFMs has the potential to enhance electrochemical performance significantly and should be studied further in future research. This approach could lead to improvements in power density by enhancing rate capability and facilitating metal-ion diffusion kinetics. There is an opportunity in this domain to advance Ni-rich cathodes through the combined design of materials involving dual cation doping (Mg^{2+}, Al^{3+}, Ti^{4+}, and Mo^{6+}) and mixed ion doping (F^-).

(iii) Additionally, exploring novel approaches such as advanced characterization techniques and computational modeling could provide deeper insights into the mechanisms underlying the improved stability and reversible capacity observed in these cathode materials. For instance, advancements in *in situ* and operando characterization techniques are pivotal for acquiring real-time insights into the reaction mechanisms and degradation processes of electrode materials and electrolytes.[39] Among these techniques, spectroscopic methods utilizing synchrotron light sources, such as X-ray absorption near edge structure (XANES), extended X-ray absorption fine structure (EXAFS), and Resonant inelastic X-ray scattering (RIXS), hold significant importance.[39] Additionally, mass spectrometry, as well as Raman and FT-IR spectroscopy, serve as powerful tools for assessing the stability of electrodes and electrolytes.[40] Furthermore, in-depth research on *in situ* electron microscopy is warranted. For example, conducting an *in situ* examination of morphological and structural evolution under varying temperature conditions can provide valuable insights into the synthesis of Ni-rich layered cathodes, especially when monitored by electron energy loss spectroscopy (EELS).

In short, the recent advancements in employing Ni-rich layered cathode electrode materials in SIBs demonstrate promising progress, mirroring established trends and invoking a sense of déjà vu. This reinforces the strong potential for global adoption of these SIB technologies. However, there is still considerable work ahead to meet the energy demands of our society.

Conflicts of interest

There are no conflicts to declare.

Acknowledgements

The authors wish to convey their profound gratitude for the substantial financial backing rendered by several distinguished Brazilian funding agencies, namely, the São Paulo Research Foundation (FAPESP 2017/11986-5), the Brazilian Innovation Agency (FINEP), the Foundation for Research Development (FUNDEP), and the National Council for Scientific and Technological Development (CNPq, Grant #405643/2022-5). This indispensable support has played an instrumental role in facilitating the successful execution of our research endeavors. J. M. G acknowledges funding through MACKPESQUISA (Fundo Mackenzie de Pesquisa e Inovação; Grant # 231020, MACK – 0012774/00). Furthermore, we wish to extend our heartfelt appreciation to Shell for their unwavering commitment and valuable support throughout this study. In addition, we would like to acknowledge the strategic significance of the unwavering assistance provided by the Brazilian National Oil, Natural Gas, and Biofuels Agency (ANP) through the Research and Development (R&D) levy regulation.

References

1 P. Zhou, X. Liu, J. Weng, L. Wang, X. Wu, Z. Miao, J. Zhao, J. Zhou and S. Zhuo, *J. Mater. Chem. A*, 2019, **7**, 657–663.

2 H. Huang, X. Wu, Y. Gao, Z. Li, W. Wang, W. Dong, Q. Song, S. Gan, J. Zhang and Q. Yu, *Adv. Energy Mater.*, 2024, 2304251.

3 Y. Liu, Y.-H. Zhang, J. Ma, J. Zhao, X. Li and G. Cui, *Chem. Mater.*, 2024, **36**, 54–73.

4 Y. Gupta, P. Siwatch, R. Karwasra, K. Sharma and S. K. Tripathi, *Renewable Sustainable Energy Rev.*, 2024, **192**, 114167.

5 B. Xiao, Y. Zheng, M. Song, X. Liu, G.-H. Lee, F. Omenya, X. Yang, M. H. Engelhard, D. Reed, W. Yang, K. Amine, G.-L. Xu, P. B. Balbuena and X. Li, *Adv. Mater.*, 2023, 2308380.

6 L. Chang, R. Yang, X. Bi, W. Yang, K. Cai, A. Wei and J. Liu, *J. Energy Storage*, 2023, **73**, 109025.

7 S. Zhao, Q. Shi, W. Feng, Y. Liu, X. Yang, X. Zou, X. Lu and Y. Zhao, *Carbon Neutrality*, 2023, **2**, 13.

8 J. L. Pimlott, R. J. Street, M. P. Down and C. E. Banks, *Adv. Funct. Mater.*, 2021, **31**, 2107761.

9 K. Mathiyalagan, D. Shin and Y.-C. Lee, *J. Energy Chem.*, 2024, **90**, 40–57.

10 S. Li, Y. Sun, Y. Pang, S. Xia, T. Chen, H. Sun, S. Zheng and T. Yuan, *Asia-Pac. J. Chem. Eng.*, 2022, **17**, e2762.

11 A. Kanwade, S. Gupta, A. Kankane, M. K. Tiwari, A. Srivastava, J. A. Kumar Satrughna, S. Chand Yadav and P. M. Shirage, *RSC Adv.*, 2022, **12**, 23284–23310.

12 S. Xu, H. Dong, D. Yang, C. Wu, Y. Yao, X. Rui, S. Chou and Y. Yu, *ACS Cent. Sci.*, 2023, **9**, 2012–2035.

13 X. Li, Y. Fan, B. Johannessen, X. Xu, K. W. See and W. K. Pang, *Batteries Supercaps*, 2024, e202300618.

14 F. Wei, Q. Zhang, P. Zhang, W. Tian, K. Dai, L. Zhang, J. Mao and G. Shao, *J. Electrochem. Soc.*, 2021, **168**, 050524.

15 W. Zuo, A. Innocenti, M. Zarrabeitia, D. Bresser, Y. Yang and S. Passerini, *Acc. Chem. Res.*, 2023, **56**, 284–296.

16 Y. Zhao, Q. Liu, X. Zhao, D. Mu, G. Tan, L. Li, R. Chen and F. Wu, *Mater. Today*, 2023, **62**, 271–295.

17 T. Chen, B. Ouyang, X. Fan, W. Zhou, W. Liu and K. Liu, *Carbon Energy*, 2022, **4**, 170–199.

18 C. Delmas, C. Fouassier and P. Hagenmuller, *Physica B+C*, 1980, **99**, 81–85.

19 N. Yabuuchi, K. Kubota, M. Dahbi and S. Komaba, *Chem. Rev.*, 2014, **114**, 11636–11682.

20 P.-F. Wang, Y. You, Y.-X. Yin and Y.-G. Guo, *Adv. Energy Mater.*, 2018, **8**, 1701912.

21 Q. Liu, Z. Hu, W. Li, C. Zou, H. Jin, S. Wang, S. Chou and S.-X. Dou, *Energy Environ. Sci.*, 2021, **14**, 158–179.

22 P. Venkatachalam, C. Karra, K. K. Duru, P. S. Maram, A. A. Madhavan and S. Kalluri, *J. Electrochem. Soc.*, 2022, **169**, 070536.

23 V. P. Mhaske, S. Jilkar and M. D. Yadav, *Energy Fuels*, 2023, **37**, 16221–16244.

24 N. G. Garcia, J. M. Gonçalves, C. Real, B. Freitas, J. G. Ruiz-Montoya and H. Zanin, *Energy Storage Mater.*, 2024, **67**, 103213.

25 X. Gao, X. Zhang, X. Liu, Y. Tian, Q. Cai, M. Jia and X. Yan, *Small Methods*, 2023, **7**, 2300152.

26 F. Ding, C. Zhao, D. Zhou, Q. Meng, D. Xiao, Q. Zhang, Y. Niu, Y. Li, X. Rong, Y. Lu, L. Chen and Y.-S. Hu, *Energy Storage Mater.*, 2020, **30**, 420–430.

27 J.-Y. Hwang, S.-M. Oh, S.-T. Myung, K. Y. Chung, I. Belharouak and Y.-K. Sun, *Nat. Commun.*, 2015, **6**, 6865.

28 J.-Y. Hwang, S.-T. Myung, C. S. Yoon, S.-S. Kim, D. Aurbach and Y.-K. Sun, *Adv. Funct. Mater.*, 2016, **26**, 8083–8093.

29 J.-Y. Hwang, S.-T. Myung, J. U. Choi, C. S. Yoon, H. Yashiro and Y.-K. Sun, *J. Mater. Chem. A*, 2017, **5**, 23671–23680.

30 H.-H. Sun, J.-Y. Hwang, C. S. Yoon, A. Heller and C. B. Mullins, *ACS Nano*, 2018, **12**, 12912–12922.

31 T.-Y. Yu, J.-Y. Hwang, I. T. Bae, H.-G. Jung and Y.-K. Sun, *J. Power Sources*, 2019, **422**, 1–8.

32 L. Zheng, R. Fielden, J. C. Bennett and M. N. Obrovac, *J. Power Sources*, 2019, **433**, 226698.

33 M. Li, X. Qiu, Y. Yin, T. Wei and Z. Dai, *J. Alloys Compd.*, 2023, **969**, 172406.

34 B. Peng, Z. Zhou, J. Shi, X. Huang, Y. Li and L. Ma, *Adv. Funct. Mater.*, 2024, 2311816.

35 X. Wang, G. Liu, T. Iwao, M. Okubo and A. Yamada, *J. Phys. Chem. C*, 2014, **118**, 2970–2976.

36 J.-Y. Hwang, C. S. Yoon, I. Belharouak and Y.-K. Sun, *J. Mater. Chem. A*, 2016, **4**, 17952–17959.

37 J. Yang, M. Tang, H. Liu, X. Chen, Z. Xu, J. Huang, Q. Su and Y. Xia, *Small*, 2019, **15**, 1905311.

38 X. Li, L. Liang, M. Su, L. Wang, Y. Zhang, J. Sun, Y. Liu, L. Hou and C. Yuan, *Adv. Energy Mater.*, 2023, **13**, 2203701.

39 J. M. Gonçalves, A. L. Hennemann, J. G. Ruiz-Montoya, P. R. Martins, K. Araki, L. Angnes and R. Shahbazian-Yassar, *Coord. Chem. Rev.*, 2023, **477**, 214954.

40 R. Venâncio, R. Vicentini, M. J. C. Pinzón, D. A. Corrêa, A. N. Miranda, A. C. Queiroz, F. T. Degasperi, L. J. A. Siqueira, L. M. Da Silva and H. Zanin, *Energy Storage Mater.*, 2023, **62**, 102943.